Small-scale Energy Harvesting

A research study for powering wearables

Petter Haugen

Sensor Systems project

Department of Technology
Norwegian University of Science and Technology
and
Mid Sweden University
Autumn 2016

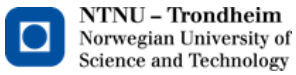

Summary

This report is a research study, which examines energy harvesting for wearables, and in particular smartwatches. Literature mainly from universities and research centers is examined to determine if a smartwatch can be powered by harvested energy.

The amount of harvestable energy that is available from specific human activites and regular daybased movement patterns is examined. How the physical placement of a harvester affects the amount of available energy is also considered.

Technologies that can harvest energy from human motion are briefly explained. The best suited motion based harvesting technology is indicated by comparing pros and cons for the specific solutions.

Technologies for harvesting other energies available in human presence, such as heat, solar power and radio waves are also briefly explained and discussed. Examples of realised harvesting systems are given.

The energy consumption of a particular smartwatch is examined and discussed. The power consumption is compared with the possible harvestable energy, and a conclusion is drawn from the gathered data.

For this study, the energy available from human motion is not able to power the examined smartwatch. The harvested mean power is too low due to non-deterministic use, and harvester location and optimization is also playing an important role. The solar and thermoelectric harvesting solutions displayed in this study are able to harvest more energy at human interaction, but will neither be able to power the same smartwatch.

Further developments in silicon technology is likely to increase the effectiveness for certain forms of energy harvesting. When the solutions under development have a huge commercial value to the involved players, the research material available for outsiders is limited.

Contents

List of Tables

List of Figures

Chapter 1

Introduction

Today people are surrounded by sensors integrated in smartphones, bracelets and similar, and we like to bring them wherever we are because of their size and ease of use. An item attached to or near-bound to our body, communicating with a smartphone or similar device can be defined as a wearable.
Even though most wearables offer power efficient computing and wireless communication, their battery capacity is known to be poor, varying from 1 day up to approximately 1 week between each recharge cycle for most wearables.
Human activity involves some form of energy trading. Workouts at the gym, walking to the office and other activities are based upon humans doing work on their surroundings.
What if the energy related to these activities could be harvested and power any smart device involved in the activity? And what if the energy harvesting service was integrated in the smart device, making proprietary charging solutions unnecessary?
This research study explores research literature involving the harvesting technologies that are most suitable for human energy harvesting, and how this energy can be exploited into smart wearables.
The main goal of the study is to answer these criterions:

- How much energy can be harvested from human motion, when the user has a normal activity pattern during one day?
- Which technology is best suited for human energy harvesting, when it should maximize power generation and be integrated in a small wearable device, e.g. a smartwatch?
- What is the general power consumption of a wearable device, e.g. a smartwatch, and how does the power consumption correspond to the available harvested energy rate?

Chapter 2

Human energy harvesting

2.1 Human motion studies - kinetic energy harvesting

2.1.1 Kinetic energy - Theory

Human motion can be viewed as kinetic energy, which represents possible work that objects can do because of their motion. Kinetic energy has the following definition:

$$K_e = \frac{1}{2} \times mass \times velocity^2 \tag{2.1}$$

Since the work conducted by human motion consists of non-constant speed, a more suitable parameter to measure is the acceleration related to those motions. By integrating the acceleration value over a specific time, we can find the velocity and the kinetic energy available for that time.(D Young and A Freedman, 2012)

$$K_e(t) = \frac{1}{2} \times m \times [v(t)]^2 = \frac{1}{2} \times m \times (\int_{t=0}^{t} adt)^2 \tag{2.2}$$

This is a simplified mathematical expression to relate acceleration and kinetic energy. More extensive algorithms will most likely calculate the data from realized measurement and harvesting systems, and I will not use time to explain such an algorithm in detail. These algorithms will also account for parameters such as data modelling and contribution from other physical properties, to give the most realistic measurement.

2.1.2 Kinetic energy - Mass-spring-damper model

A kinetic energy harvesting system can be modelled mathematically to configure the systems overall behavior and express the available energy. A mass-spring-damper modeled harvester is depicted in **Figure 2.1**. Intertial-force generators, as depicted in **Figure 2.1**b is preferred as vibration energy harvesters since they only need one point of attachment to the vibrating/moving structure. (Vocca and Cottone, 2014)

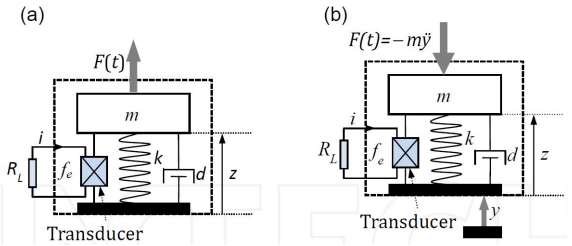

Figure 2.1: Mass-spring-damper modeled force generators. a) Direct-force b) Intertial-force

The k and d parameters of **Figure 2.1** represents the parameters of the harvesting system being able for optimization. Such parameters are typically resonant frequency and quality factor. The mathematical model to determine these parameters will be dependent of the harvester architecture. Vocca and Cottone (2014) shows a mathematical model of a kinetic harvesting system, and how selection of k and d parameters affects the overall performance of such a system.

2.1.3 Columbia University study - Test setup

A study performed at Columbia University focuses on the energy available from human motion to power IoT nodes. The study uses two data sets, which contains acceleration data for specific physical activities from over fourty participants, and long-term human motion tracking from five participants. The acceleration data is obtained with two separate measurement systems, containing tri-axis accelerometers and data loggers. The accelerometers are located at three specific locations on the body, and the orientation of each accelerometer is not controlled.

The acceleration data is modelled as a second-order mass-spring system, with similarities to the system depicted in **subsection 2.1.2**. The k and d parameters of the system are optimized for each test setup, to maximize the available energy. The k and d parameters are chosen for each test setup after executing an exhaustive search algorithm.

The overall acceleration magnitude from the three axis is computed and filtered for gravitational contribution. The average absolute deviation of acceleration (AADA) and dominant frequency of motion are extracted and further examined to determine the energy available from each data set. (Gorlatova et al., 2014)

2.1.4 Columbia University study - Physical activity

As earlier mentioned, the research group studied a data set containing acceleration data for seven specific activities: relaxing, walking, fast walking, running, cycling, going up- and downstairs. **Figure 2.2** and **Table 2.1** depicts parts of the extracted information from the 40-participant dataset. The three data points for each activity are close; meaning the placement of the sensor was slightly irrelevant for this study. On the other hand, all of the sensors in this study are placed on or nearby the torso. Comparing with sensors located on the wrists or ankles could give differing results. (Gorlatova et al., 2014) The results also confirms that kinetic energy is more dependent of AADA instead of frequency. This is shown in **Figure 2.2**, where two of the cycling frequency data points are the highest in the entire study, but the energy harvested is low compared with other activities such as walking or running. As earlier mentioned, placing a sensor on the candidates' ankles could have improved the harvesting result sufficiently.(Gorlatova et al., 2014)

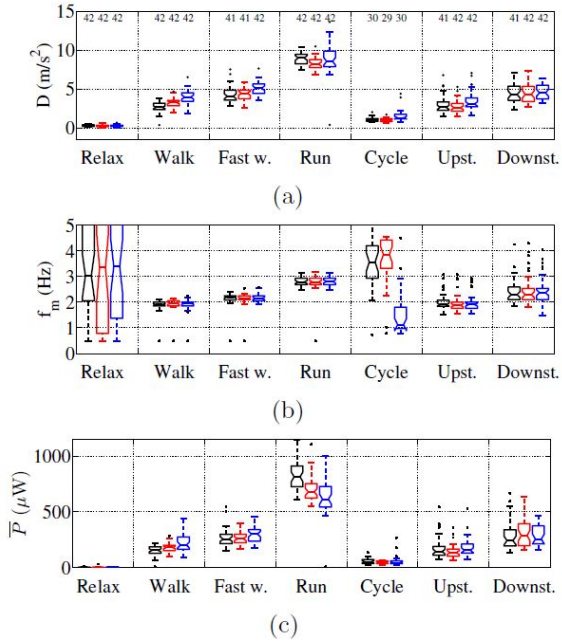

Figure 2.2: Kinetic energy characterization for common human activities. a) Average absolute deviation of acceleration. b) Dominant motion frequency. c) Power harvested by an optimized harvester.
Accelerometer locations: Black: shirt pocket. Red: waist belt. Blue: trouser pocket

As **Table 2.1** depicts, the average power harvested in a walking session is in the interval 150 to 200 uW if the median value is considered. The median value in a running session is significantly higher, in the interval 600 to 800 uW. Note that the motion frequency for running is 2.8 Hz, compared to 2 Hz for walking. When the harvester is optimized for each activity, using the same parameters for

Table 2.1: Energy characterization for human activities

Activity	Sensing unit placement	# subjects	Median f_m (Hz)	$\overline{P}$ (μW)			Median r (Kb/s)
				25th percentile	Median	75th percentile	
Relaxing	Trouser pocket	42	N/A	1.0	3.1	4.8	0.6
	Waist belt	42	N/A	0.3	2.4	4.8	0.5
	Trouser pocket	42	N/A	0.2	1.4	5.9	0.3
Walking	Shirt pocket	42	1.9	128.6	155.2	186.0	31.0
	Waist belt	42	2.0	151.8	180.3	200.3	36.0
	Trouser pocket	42	2.0	163.4	202.4	274.5	40.4
Running	Shirt pocket	42	2.8	724.2	813.3	910.0	162.6
	Waist belt	41	2.8	623.5	678.3	752.8	135.6
	Trouser pocket	42	2.8	542.3	612.7	727.4	122.5
Cycling	Shirt pocket	30	3.5	37.4	52.0	72.3	10.4
	Waist belt	29	3.8	36.3	45.4	59.2	9.1
	Trouser pocket	30	1.1	35.6	41.3	59.5	8.3

the walking and running harvesters would possibly decrease the harvested power for one of the activities, depending on the parameter in use.

2.1.5 Columbia University study - Long term human motion tracking

The research group also studied a dataset consistent of acceleration data for a longer time. The study's five participants carried a sensing unit at a freely chosen place at their body, and wore the unit for a longer period of time, typically from morning to evening. All of the participants had normal activity patterns, such as walking to the office, walking to meetings, other arrangements etc. **Table 2.2** depicts key parameters of the dataset, such as the time spent with the unit, activity pattern and harvested energy. As **Table 2.2** depicts, the mean power harvested when the unit is worn an entire day is dramatically lower for this dataset than the 40 participant set. $\overline{P}_{avg}$ is the average power harvested during the entire time interval, while $\overline{P}_{d_{avg}}$ is the average power a harvester would have generated over a 24 hour interval. $\overline{P}^{H4}_{avg}$ is the average harvested power for each user when a common optimization pattern is applied. The harvesters are optimized for participant M4's dominant frequency of motion, and as a result the possible harvested power is even lower. Since a wearable device, such as a smartwatch won't be worn at the body at all times, and a common optimized harvester is the most likely implementation, $\overline{P}_{d_{avg}}$ and $\overline{P}^{H4}_{avg}$ are the two calculations that probably will be the best representation of possible energy harvesting from such systems.

Table 2.2: Energy characterization for prolonged human activity

Participant	Occupation and commute	# days	Total dur. (h)	Optimized harvester		r_d, avg (Kb/s)	$\overline{P}^{H4}$ (μW), min/avg/max	% ON, min/avg/max
				$\overline{P}$ (μW), min/avg/max	$\overline{P}_d$ (μW), min/avg/max			
M1	Undergraduate student, male, living on campus, always goes to the lab	5	60.4	6.9 / 13.8 / 17.3	4.8 / 6.5 / 8.1	1.3	5.0 / 8.5 / 10.9	5.4 / 9.9 / 12.2
M2	Undergraduate student, male, commuting to campus, always goes to the lab	3	27.7	23.3 / 29.0 / 38.2	8.4 / 11.5 / 17.7	2.3	17.1 / 19.6 / 24.5	13.6 / 16.1 / 18.4
M3	Undergraduate student, female, living on campus, sometimes works from home	9	62.0	2.4 / 7.16 / 13.4	0.6 / 2.02 / 3.6	0.4	2.0 / 5.8 / 12.2	3.6 / 6.0 /9.95
M4	Graduate student, female, commuting to campus, sometimes works from home	7	80.1	1.4 / 11.98 / 25.3	0.6 / 5.6 / 10.7	1.1	1.4 / 11.98 / 25.3	2.8 / 12.7 / 18.1
M5	Software developer, male, commuting to office, always goes to the office	1	11.0	16.3	7.5	1.5	15.9	11.5

Figure 2.3 depicts the AADA and harvested energy during a normal day for participant M5. The energy is harvested in small timeslots a few times per day,

consistent with the walking pattern of participant M5. For comparison, **Figure 2.4** depicts the relationship between the total energy harvested and each power level, as well as how much of the total time each power level has been harvested at. For 91 percent of the total time the energy harvested is in the interval 0 to 15 uW. (Gorlatova et al., 2014)

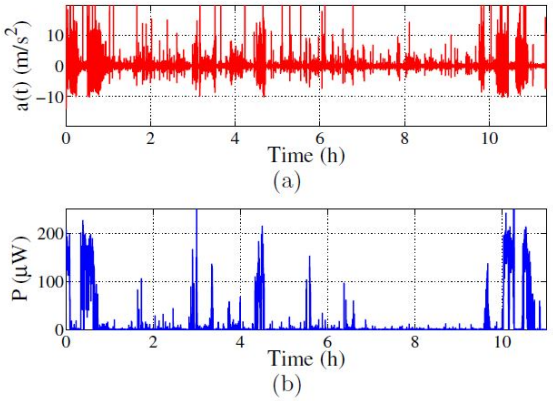

Figure 2.3: Kinetic energy in a normal daily routine. a) Acceleration scope during an 11-hour trace. b) Harvested energy during the same time scope.

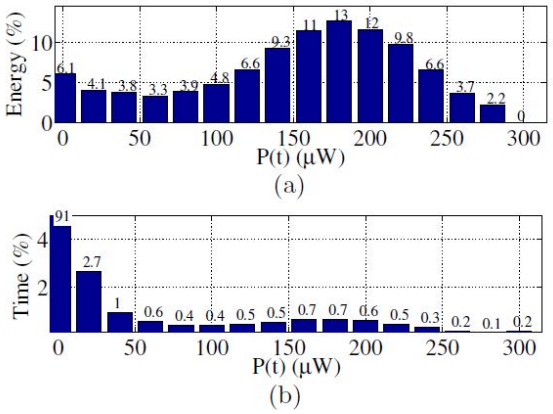

Figure 2.4: Energy harvesting variability. a) Percentage of total energy harvested. b) Percentage of time the power is harvested at each p (t).

2.1.6 University of Southampton study - The efffect of sensing unit location

A study performed at the University of Southampton focuses on sensor unit location and orientation for human-powered energy harvesting. The test group consist of

ten participants which are told to walk and run at a comfortable rate. Five sensing units containing tri-axis accelerometers are located at five specific locations on their body. The researchers has calculated the maximum output power and relative power from the acceleration data, as shown in the equations beneath.

$$P = \frac{mA^2}{8\pi f_0 \epsilon} \tag{2.3}$$

$$P_r el = \frac{A^2}{8\pi f_0} \tag{2.4}$$

The relative power is examined to determine the energy available at each sensing unit location, as shown in **Figure 2.5**. The main findings from the study is that the power generated from the lower part of the body is approximately one order higher than the upper part, such as wrist and waist. The relative power is more even when running, probably because of increased upper body activity while running. (Huang et al., 2011)

Note: **Figure 2.5** might give the impression that the energy available from this experiment is in the range of multiple watts, considering the weight of a human being. The actual mass from the human body making an impact on the harvester is microscopic, and the energy available is in the uW-range, according to Huang et al. (2011).

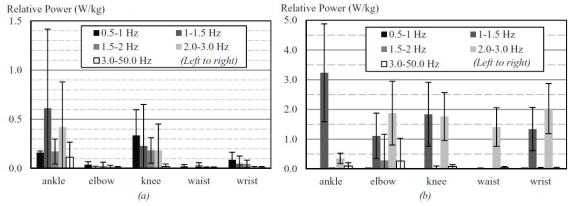

Figure 2.5: Relative power available for different sensing locations a) Walking b) Running

Chapter 3

Harvesting technologies

3.1 Kinetic energy - Piezoelectric absorption

3.1.1 The piezoelectric effect

The piezoelectric effect refers to a change in the electric field of a certain crystalline material when mechanical stress is applied. The change of electric field is due to the non-centric-symmetric crystal structure of the material. By placing the center ion slightly off center, each related unit cell is turned into an electric dipole. By poling each unit cell, the dipoles are manipulated to orient in slightly the same direction, as shown in **Figure 3.2** b. When mechanical stress is applied to the material, the position of each center element in all of the unit cells is shifted in the same direction, maximizing the force of the generated electric field. (Multiphysics-Cyclopedia, NKb) This process is reversible, meaning that applying an electric field to a certain material can generate a mechanical deformation. (Multiphysics-Cyclopedia, NKa) **Figure 3.1** depicts the electric field in a piezoelectric Quartz lattice at three situations, where the electric field changes according to the force applied to the material.

3.1.2 The piezoelectric transducer

The crystal orientation is together with material selection the key components in piezoelectric transducer design. The best known material for piezoeletric energy harvesting is lead zirconate titanate (PZT), due to its high piezoelectric constant. (Hudak and Amatucci, 2008) **Figure 3.2** a depicts how the crystal can be oriented to absorb force in either longitudinal or transverse direction. **Figure 3.2** c shows a piezoelectric cantilever beam sensor, operating in 31 mode with a weight placed on the freely moving part of the crystal, maximizing the impact of the applied force and hence also the electric field.

Piezoelectric transducers are available as both single- and multilayer construc-

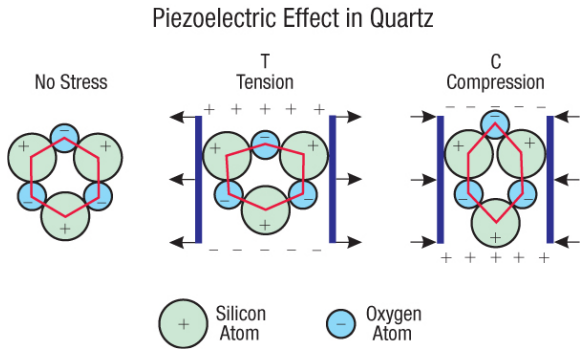

Figure 3.1: Piezoelectric characteristic

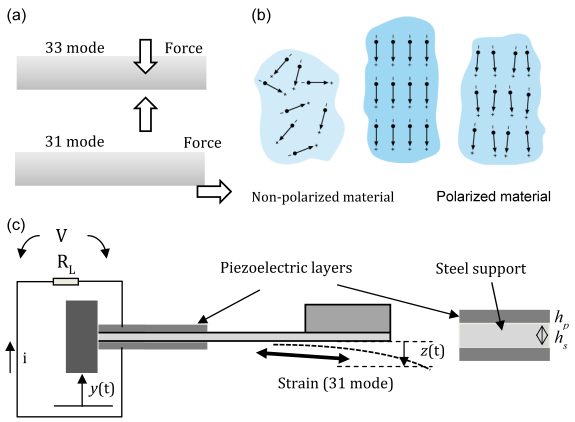

Figure 3.2: a) Longitudal and transverse stress absorption b) Polarization scheme for crystals c) Piezoelectric cantilever beam

tions. The construction of the transducer will often be dependent of the absorption direction. The classical construction method is a protective coating for single- or multilayer constructions, and wires to connect the transducer to a rectifier and charge control system. Such constructions are often found both as harvesting systems implanted in shoe soles, and as actuators found in fire alarm buzzers. Piezoelectric transducers can also be constructed as MEMS devices, offering energy harvesting, rectification, voltage controller and possibly a microcontroller, integrated in one single chip. With a significantly smaller chip size than the earlier mentioned setup, they are well suited for use in areas where size matters.

Vocca and Cottone (2014) claims that the available power is significantly higher for a 33-mode absorption system compared to a 31-mode system, due to the possible strain and coupling coefficients of the 33-mode system. On the other hand, the 33-mode system is best suited for high frequency operations, while a 31-mode system easier can produce an electric charge after being suppressed to strain at

lower frequencies. Conventional MEMS devices are mostly constructed as 31 mode harvesters, with a piezoelectric layer placed between the top and bottom electrode. The voltage generated from this system is proportional to the piezoelectric constant, applied stress and the thickness of the piezoelectric layer. Kim et al. (2012) claims that with today's technology both the piezoelectric constant and acceleration in a typical 31 mode use case is too low to generate a voltage passable for a rectifying circuit. Studies done by Jeon et al. shows that 33 mode-harvesting systems are the most advantageous today. Future advancements in piezoelectric technology will eventually enable the use of 31-mode piezoelectric materials with higher material constants. Piezoelectric materials of this kind will help realizing future 31-mode MEMS harvester solutions. (Kim et al., 2012)

3.2 Solar harvesting

3.2.1 The photovoltaic effect

The photovoltaic effect explains how electrons and holes can generate a electromotive force by applying light at a pn-juntion. In general, semiconductor materials are doped so there is one side consistent of holes and one with electrons. Together they make an internal electric field. When light photons enter the pn-junction, electron and hole pairs are created in proximity of the junction. The pairs are then separated, electrons at the n-type and photons at the p-type semiconductor. Adding an external circuit to let the holes and electrons recombine will result in a current flow through the circuit. (Boer, 2016) (Matsushita Battery Industrial Co., 1998/1999)

3.2.2 Solar panel implemented in smartwatches

A study performed in University of Bologna and Integrated Systems Laboratory in Zurich have looked upon solar powering of smartwatches, sensor implementation and power efficiency. They have prototyped a solar powered smartwatch consistent of eight flexible solar modules, depicted in **Figure 3.3**. A detailed description of the smartwatch architecture follows:

- Flexible 40 mAh lithium rechargeable battery as storage device
- 8 pieces of AM-1471CA amorphous silicon solar panels from Sanyo Energy, connected in parallel
  Dimensions: $35 * 14[mm]$ Total area: $39cm^2$
- Voltage and current delivery from solar panels in parallell connection:
  - Indoor: I = $100uA$ @ V = $1.9V$
  - Outdoor: I = $15mA$ @ V = $1.6V$
- Energy aquired from indoor daytime use: $502uW$

- Energy aquired from outdoor daytime use: $4000uW$
- Power management IC: Texas Instruments BQ25570
- Smartwatch microcontroller: Texas Instruments MSP430FR5969
- Wireless interface: ST Microelectronics M24LR16E-R
- Sensing units: 16 NTC thermistors mounted in array

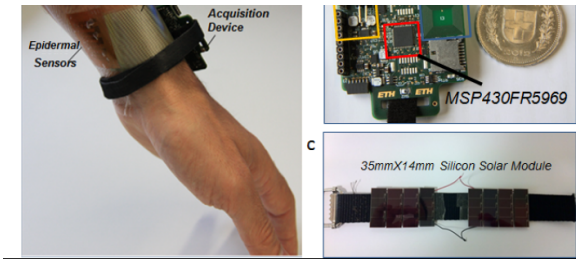

Figure 3.3: Prototyped solarpowered smartwatch

The main goal of this experimental setup is to prove if a solar powered smart watch can measure temperature data from the body, process the data and transmit them to a remote host. To make the power consumption as low as possible, the smartwatch microcontroller is configured with five modes to control the power consumption. Temperature sampling is performed once per hour, and NFC data transfer is performed every four hours. With this particular setup, the energy consumption for an entire day is estimated to be $620,38mJ$. With an average energy generated from the solar panels for indoor use of $620mJ$, this system can be self-sustainable, both for indoor and outdoor use (Magno et al., 2016)

3.3 Thermoelectric absorption

3.3.1 The Seebeck effect

The seebeck effect demonstrates how a temperature difference between two dissimilar conductors formed as a thermocouple can produce an electromotive force. The magnitude of the electromotive force is proportional to the temperature difference between the two sides of the thermocouple. The Seebeck effect can also be reversed, inducing a heating or cooling effect between two junction points, better known as the Peltier effect. These two effects are possible because electrons can possess different energy levels for different materials. By heating one of the thermal junctions, electrons are allowed to enter a material where they have a higher energy level, resulting in a electromotive force. (Goldsmid, 2010)

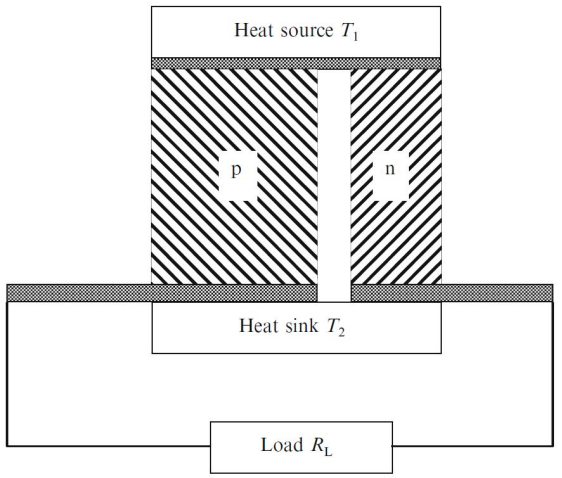

Figure 3.4: Thermoelectric energy harvester

3.3.2 Thermoelectric harvester

Figure 3.4 depicts a thermocouple and a load resistance. In a realized harvesting circuit, a charge controller would represent the load resistance. The power delivered from the thermocouple is dependent of the current generated and the load resistance.

$$W = I^2 \times R_L = [\frac{(\alpha_p - \alpha_n)(T_1 - T_2)}{R_p + R_n + R_L}]^2 \times R_L \tag{3.1}$$

A thermal harvesting system will also consist of non-ideal parameters. Parts of the applied heat will balance the Peltier cooling that occurs when a current flows in the system. Resistive heating along the two sides of the thermocouple will also represent a certain heat loss. The heat rate drawn from the source is defined as

$$q_1 = (\alpha_p - \alpha_n) \times I \times T_1 + (K_p + K_n)(T_1 - T_2) \tag{3.2}$$

The relationship between the heat applied to the system vs the power delivered to the load is w/q_1 .

To maximize power efficiency the load resistance should be matched to the generator resistance. For an ideal situation with matched resistance and no thermal losses, the efficiency would not exceed 50 % . (Goldsmid, 2010)

3.3.3 Realized thermoelectric small-scale harvester

As far we know, there has only been two wristwatches commercially available that are powered by thermoelectricity. One of them was manufactured by Seiko, and released in 1998. A picture of the watch and a principle sketch of its operation is shown in **Figure 3.5**

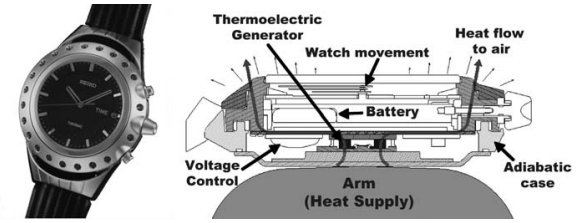

Figure 3.5: Seiko Thermoelectric watch - Prinicipal sketch

A research article written by Seiko explains the main features of the watch in more detail (Kishi et al., 1999)

- Rechargeable lithium ion battery of 1.5 V and 4.5 mAh
- Metal back casing, plastic insulated frame and top metal casing
  Heat is absorbed at the metal back casing and directed to the thermoelectric junction.
  The top metal casing acts as the second thermoelectric junction, and the insulated frame prevents possible heat loss through the frame
- Thermoelectric material: Bi-Te (Bismuth – Tellurium)
- High thermal resistance of the TE generator to maximize temperature difference: $600K/W$
- Internal resistance of TE generator: 1000 ohms
- 104 thermic elements inside each module, each capable of $200uV/K$
  10 modules connected in series, giving a total estimated voltage of $20mV/K$
- Thermoelectric harvester size: $2 \times 2 \times 1,3[mm]$
- Switched capacitor booster circuit implemented to boost the input voltage equal to the battery voltage.
  Input: 150 mV Output: 1.5 V
- Estimated maximum electrical power: $22.5uW$
- Typical electrical wristwatch consumption: $1uW$

A series of experiments was conducted to control the charge capability of the harvester system. The thermoelectric generator had reached stationary conditions with an applied input voltage for the regulator of 300 mV after approximately 30 minutes. A sufficient temperature difference between the skin and ambient is needed to drive the regulator effectively. Studies done by Blazquez et al. (2012) shows that the mean skin temperature at the wrist of a human being is in the range $[306 - 308]K$. For this particular setup, the thermoelectric generator is able to drive the watch and charge the battery at ambient temperatures below 301 K. (Kishi et al., 1999)

3.3.4 Future thermoelectric harvesting solutions

A study performed at the State University of New Jersey discusses how future thermoelectric harvesting solutions should be manufactured and implemented. Their conclusion is that researchers need to pay more attention to the fabrication process, and increasing the thermoelectric efficiency of the material, instead of focusing on the phonon loss component of thermal conductivity (Hudak and Amatucci, 2008). By now, Bismuth – Tellurium is the best suited material for small scale thermoelectric harvesting. Research covered in the article claims that improvements in the crystal growth process can give Bismuth – Tellurium combinations with higher power densities.

3.4 Radio wave absorption

3.4.1 Radio wave absorption research

A research group at the State University of New Jersey is looking at the electrical effect of radio frequency absorption. Radio frequency radiation is typically determined by the electric field strength, known as $E = volts/meter$. By considering the radiation as a plane wave, the electric field strength can be converted to represent the incident power density, known as $S = \frac{E^2}{R}[\frac{W}{m^2}]$, where R is the radiation resistance in free space.

Several sources of radio frequency was explored to determine the available power in different frequency and distance areas. A citizen area in 3 km radius of a 15 antenna cluster setup was explored. The frequency range was 55-687 MHz and the total power emitted was 9 MW. The average power densities measured inside and outside of the 161 contestants homes were 0.8 and 2.6 $\frac{uW}{cm^2}$

The frequency commitment from wireless networks was also explored. Since they operate in the ISM band, it is a possibility that the energy available here is bigger and more accessible, since most families and businesses have one or more wireless devices operating in this frequency band. A test setup was configured to measure the power densities at certain distances away from wireless equipment operating in the 2.4 GHz area, and with transmission power limited to 100 mW. At 0.5 and 2 meters distance, the power densities was measured to be 1 and 0.1 $\frac{uW}{cm^2}$.

The main conclusions of this particular study is that the energy available from radio frequencies is too small to power wireless sensor systems today. The energy is both too inaccessible and frequency dependent.(Hudak and Amatucci, 2008)

Chapter 4

Wearables

4.1 Defining a wearable

Wearables has been subject to R & D for a long time, but the definition of a wearable has been somewhat unclear if one looks back. Wearables and in particular wearable computing seems to have been defined by limitations in the current technology and/or particular application. Mann (1997) defined the wearable computer for his paper as a data processing system attached to the body, with one or more output devices. The output should be perceptible constantly despite the particular task or body position, and the input channel(s) should allow the functionality of the data processing system to be modified. This definition is still applicable for many of todays wearables, and with further R & D in the respective field, the definition of a wearable is likely to be changed even further.

4.2 Smartwatch energy consumption

The energy consumption of a modern wearable device, such as a smartwatch is highly dependent of its hardware setup and use case. To get a scope of the energy consumption for such a wearable, the specifications from several manufacturers was explored, trying to give hints regarding the energy consumption. Most of the data found from producers such as Polar, FitBit and Samsung only contained limited information about the charge cycle, and did not say anything particular about the energy consumption.

4.2.1 Indiana University studies - Energy Consumption in smartwatches

A study performed at Indiana University explores the energy consumption of smartwatches, in particular the LG Urbane watch. The LG Urbane watch has the fol-

lowing specs:

- Operating system: Android Wear
- Processor: Cortex A7
- Storage and memory: 4 GB / 512 MB
- Display: 1.3 inch P-OLED
- Wireless interfaces: Wi-Fi, Bluetooth
- Sensors: Gyroscope, accelerometer, compass, barometer, heart rate monitor

A test group of 30 persons wore the watch in their everyday activities, and energy consumption data was collected throughout the day. The data collection was still ongoing when their report was written, so their data analysis are preliminary, but still approved to give hints regarding the energy consumption. Their main finding was that more than half of the smartwatches energy consumption was done in sleeping mode, as **Figure 4.1** depicts. This means that for over half a day, the watch will consume 10 to 23 mW, according to **Table 4.1**. The mean energy consumption for an entire day was not calculated by the research group, since their data material was preliminary. The energy consumption will anyhow vary according to the use case, if sensors, displays and communication protocols are used during a workout the power consumption would be recently higher than if the watch had been in sleep mode at the office an entire day. **Figure 4.1** also shows that the display is the main energy consumer when the watch is awake. No further research is found regarding this particular matter, but changing the colored P-OLED display with a black and white OLED display could enhance the power consumption when the watch is in the active state. The research groups' conclusions and further work is mostly based on improving the power consumption of smartwatches. (Liu and Qian, 2016)

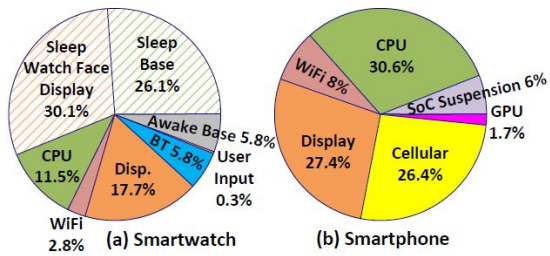

Figure 4.1: Energy breakdown of a) Smartwatch consumption b) Smartphone consumption

Table 4.1: Power consumption model for LG Urbane watch

Component	Power Consumption (mW)
Sleep (watch face off)	10.9 for the entire device
Sleep (watch face on)	23.5 for the entire device
Wakeup baseline	43.5
CPU	$184.7u - .6$, $u \in (0,1]$: CPU util.
Display (default brightness level)	$\sum(.030r + .127g + .233b + 93.7)/K$ Per-pixel $r, g, b \in [0, 255]$, K=320*320
Wi-Fi Tail	Duration: 0.18 sec, Power: 178.3
Wi-Fi Promotion	Duration: 0.30 sec, Power: 299.6
Wi-Fi Data	Tx: 739.9, Rx: 400.1
BT Tail	Duration: 4.8 sec, Power: 97.2
BT Data	Tx: 180.7, Rx: 174.9
Screen touch/swipe	118.9

4.2.2 Koreatech university studies - Battery use and management for smartwatches

A similar study has also been performed at Koreatech University. The study primarily focuses on the use and charge pattern for Android Wear smartwatches. Seventeen Android Wear smartwatch users participated in an online survey and installed an application that collected battery usage data both for their smartwatch and for smartphone. The application runs as a background service, and was active for three weeks. The battery drain rate was calculated by comparing the time stamp and battery level at consecutive times. The mean battery drain rate was calculated to be 2.3 percent of the total battery capacity per hour. This is not a recommended academic approach to define the drain rate, since the total battery capacity is non-equal for different smartwatch brands. The information collected from the study is most of all used to give an indication of the total battery capacity and expected operational time between each charge.
An interesting finding is that even if the battery capacities are unknown, the drain rate is not varying significantly. Probably the battery capacities are all approximately 400 mAh, and the smartwatches are running applications with approximately the same power consumption, even though this is not verifiable. The average operation period for all of the smartwatches in the study is estimated to be 42.8 hours. (Min et al., 2015)

Chapter 5

Discussion and conclusion

5.1 Discussion

Kinetic harvesting of energy is available in three methods: Electromagnetic vibration absorption, electrostatic vibration absorption or piezoelectric absorption. Piezoelectric absorption is by far the method that is mostly researched, documented and realized in harvester systems. A quick look at some research articles revealed that the electromagnetic and electrostatic harvesters was hence in the cm-scale of size, the latter also needed an externally applied voltage to enable harvesting. For the above-mentioned reasons these two solutions are considered not feasible, and are thus excluded from the paper.

The piezoelectric transducer can be configured and implemented in a wide variety of setups. My explanations of the transducer are the most basic ones, and there is probably a transducer setup that can extract more power out of the available motions. Because the energy available from such motions turned out to be microscopic, I did not prioritize to find such a transducer.

Some literature regarding energy harvesting with gyroscopic devices was found during the study period. The main advantage of such a device would be its independency of direction; energy could possibly be harvested in all directions. On the other hand, gyroscopes are not suited as MEMS devices, due to mechanical setbacks. A vibrating gyro has been adapted for MEMS fabrication, and is most likely to be implemented as an energy harvester in the future (Yeatman, 2008).

Solar panels are popular as energy harvesting devices, and they are used in a variety of applications, among them watches. According to Maehlum (2015), the energy efficiency of amorphous silicon is low compaired with other thin film materials, such as Cadium Telluride. Doing further research in solar cell material selection for wearables could be an interesting topic. Seiko uses amorphous silicon in their Eco-Drive watch-series, most likely because the energy available from the solar panels are sufficient to both power the watch and charge the energy storage cells (Citizen, Not known).

The energy consumption for smartwatches in this paper is based upon a few studies. Because the research material is limited, there is likely other smartwatches that has a lower energy consumption than the one discussed in **subsection 4.2.1**. Finding the energy consumption of a typical fitness tracker and compairing with a fully specified smartwatch could be an interesting topic. My prediction is that the energy consumption still would be too great to enable energy harvesting solutions with todays technology.

5.2 Conclusion

This study has explored research articles and other relevant literature to find human related energies available for harvesting. The energy available for harvesting from human motion is microscopic compared to the energy needed to power a wearable smartwatch. The mean power available for harvesting through one day was in the interval $[2 - 11uW]$. With a non-optimized harvester, the energy is even lesser. If the LG Urbane Watch from **subsection 4.2.1** is considered, a power consumption of 10 mW would be the minimum. After considering the literature for this study, it can be concluded that harvesters with a non-deterministic energy pattern such as human motion harvesters and rf harvesters are considered not usable for such matters. Even not thermal and solar harvesting solutions can power a smartwatch with the above-mentioned power consumption, when they harvest a mean power of respectively 22 uW and 502 uW. The thermal and solar harvesting solutions has a more equal supply of energy through a day, and they will at least be able to harvest a consistent energy rate throughout a full day. All in all, today's energy harvesting solutions does not have the ability to harvest all applied amounts of a specific energy, and convert this particular energy to electricity. Further advances in process engineering for development and production of semiconductors will hopefully increase the efficiency of energy harvesters and charge controllers.

Bibliography

Blazquez, A., Martinez-Nicolas, A., Salazar, F., Rol, M., Madrid, J., 2012. Wrist skin temperature, motor activity, and body position as determinants of the circadian pattern of blood pressure. Chronobiology international 29 (6), 747–756.

Boer, K., 2016. Chemistry explained.
URL http://www.chemistryexplained.com/Ru-Sp/Solar-Cells.html

Citizen, Not known. Citizen faqs, eco-drive.
URL http://www.citizenwatch.com/en-us/faq-category/eco-drive/

D Young, H., A Freedman, R., 2012. Young and Freedman University Physics 13th edition. Pearson.

Goldsmid, H. J., 2010. Introduction to thermoelectricity. Vol. 121. Springer.

Gorlatova, M., Sarik, J., Grebla, G., Cong, M., Kymissis, I., Zussman, G., 2014. Movers and shakers: Kinetic energy harvesting for the internet of things. In: ACM SIGMETRICS Performance Evaluation Review. Vol. 42. ACM, pp. 407–419.

Huang, H., Merrett, G. V., White, N. M., 2011. Human-powered inertial energy harvesters: the effect of orientation, location and activity on obtainable power. Procedia Engineering 25, 815–818.

Hudak, N. S., Amatucci, G. G., 2008. Small-scale energy harvesting through thermoelectric, vibration, and radiofrequency power conversion. Journal of Applied Physics 103 (10), 101301.

Kim, S.-G., Priya, S., Kanno, I., 2012. Piezoelectric mems for energy harvesting. MRS bulletin 37 (11), 1039–1050.

Kishi, M., Nemoto, H., Hamao, T., Yamamoto, M., Sudou, S., Mandai, M., Yamamoto, S., 1999. Micro thermoelectric modules and their application to wristwatches as an energy source. In: Thermoelectrics, 1999. Eighteenth International Conference on. IEEE, pp. 301–307.

Liu, X., Qian, F., 2016. Measuring and optimizing android smartwatch energy consumption: poster. In: Proceedings of the 22nd Annual International Conference on Mobile Computing and Networking. ACM, pp. 421–423.

Maehlum, M. A., 2015. Energy informative.
URL http://energyinformative.org/best-thin-film-solar-panels-amorphous-cadmium-

Magno, M., Salvatore, G. A., Mutter, S., Farrukh, W., Troester, G., Benini, L., 2016. Autonomous smartwatch with flexible sensors for accurate and continuous mapping of skin temperature. In: Circuits and Systems (ISCAS), 2016 IEEE International Symposium on. IEEE, pp. 337–340.

Mann, S., 1997. Introduction: On the bandwagon or beyond wearable computing? Personal Technologies 1 (4), 203–207.

Matsushita Battery Industrial Co., L., 1998/1999. Panasonic Solar Cells Technical Handbook '98/99.
URL http://solarbotics.net/library/datasheets/sunceram.pdf

Min, C., Kang, S., Yoo, C., Cha, J., Choi, S., Oh, Y., Song, J., 2015. Exploring current practices for battery use and management of smartwatches. In: Proceedings of the 2015 ACM International Symposium on Wearable Computers. ACM, pp. 11–18.

Multiphysics-Cyclopedia, C., NKa. Piezoelectric effect.
URL https://www.comsol.com/multiphysics/piezoelectric-effect

Multiphysics-Cyclopedia, C., NKb. Piezoelectric materials: Crystal orientation and poling direction.
URL https://www.comsol.com/blogs/piezoelectric-materials-crystal-orientation-po

Vocca, H., Cottone, F., 2014. Kinetic energy harvesting. ICT-Energy-Concepts Towards Zero-Power Information and Communication Technology, 25–48.

Yeatman, E. M., 2008. Energy harvesting from motion using rotating and gyroscopic proof masses. Proceedings of the Institution of Mechanical Engineers, Part C: Journal of Mechanical Engineering Science 222 (1), 27–36.